Biochem. J. (1973) 133, 209-226
Printed in Great Britain

Light-Scattering Studies on Supercoil Unwinding

By AILSA M. CAMPBELL and DOUGLAS J. JOLLY*
Institute of Biochemistry, University of Glasgow, Glasgow G12 8QQ, U.K.

(*Received* 6 *October* 1972)

It has been shown previously that supercoiled ϕX174 bacteriophage intracellular DNA (mol.wt. 3.2×10^6) with superhelix density, $\sigma = -0.025$ (−12 superhelical turns) at 25°C is best represented as a Y shape. In this work two techniques have been used to unwind the supercoil and study the changes in tertiary structure which result from changes in the secondary structure. The molecular weights from all experiments were in the range $3.2\times10^6\pm0.12\times10^6$. In experiments involving temperature change little change in the Y shape was observed between $\sigma = -0.027$ (−13 superhelical turns, 14.9°C) and $\sigma = -0.021$ (−10 superhelical turns, 53.4°C) as evidenced by the root-mean-square radius and the particle-scattering factor $P(\theta)$. However, at $\sigma = -0.0176$ (−8 superhelical turns, 74.5°C) the root-mean-square radius fell to between 60 and 70nm from 90nm indicating a large structural change, as did alterations in the $P(\theta)$ function. In experiments with the intercalating dye proflavine from values of bound proflavine of 0–0.06mol of dye/mol equiv. of nucleotide which correspond to values of σ from −0.025 to −0.0004 (−12 to 0 superhelical turns) a similar transition was found when the superhelix density was changed by the same amount, and the molecule was shown to go through a further structural change as the unwinding of the duplex proceeded. At $\sigma = -0.018$ (−9 superhelical turns) the structure was compatible with a toroid, and at $\sigma = -0.0004$ it was compatible with a circle but at no point in the sequence of structure transitions was the structure compatible with the conventional straight interwound model normally visualized as the shape of supercoiled DNA.

Circular DNA molecules now seem extremely common and widely distributed in nature (Helinski & Clewell, 1971), both in bacterial and in eukaryotic systems. A large number of DNA molecules have been shown to exist in a supercoiled form (Vinograd & Lebowitz, 1966) and it seems likely that most others do also. In addition supercoiled, but not necessarily circular, DNA has been invoked as a virus-packaging method (Kilkson & Maestre, 1962), as structural (Pardon *et al.*, 1967; Luzzati & Nicolaieff, 1963) and as functional (Crick, 1971) units in terms of gene regulation in chromosomes of higher cells.

Earliest investigations of the structure of supercoiled covalently closed circular DNA were by ultracentrifugation and electron microscopy (Kleinschmidt *et al.*, 1963; Vinograd *et al.*, 1965). These two techniques and viscosity (Revet *et al.*, 1971; Saucier *et al.*, 1971) have continued to be the tools used in the vast majority of studies on supercoiled DNA structure (Crawford & Waring, 1967; Bode & MacHattie, 1968; Bauer & Vinograd, 1968; Wang, 1969; Upholt *et al.*, 1971).

Despite these and other reports the actual three-dimensional solution structure of supercoiled DNA has remained obscure; for example, Wang (1969) found the theoretical predictions of the sedimentation coefficient by Fukatsu & Kurata (1966) and Bloomfield (1966) were inappropriate. The most comprehensive attempt to elucidate the three-dimensional structure of supercoiled DNA has been by Upholt *et al.* (1971). These workers investigated a range of superhelix density, σ (the number of superhelical turns per ten base pairs), from −0.085 to 0 by using SV40† DNA (mol.wt. 3×10^6), bacteriophage PM2 DNA (mol.wt. 6×10^6) and bacteriophage λ b_2b_5c DNA (mol.wt. 25×10^6). As indicated by the results of Wang (1969) and Dean & Lebowitz (1971) there appears to be more than one phase to the plot of sedimentation coefficient against superhelix density. Because of the inadequacies of existing theories for calculating sedimentation coefficients, Upholt *et al.* (1971) were forced to rely on electron micrographs for correlation of sedimentation coefficients with molecular structure. However, data from electron micrographs can provide artifactual results especially where the conformations are taken as an indication of solution structure. Crawford & Waring (1967),

* Present address: Polymer Research Department, Weizmann Institute of Science, Rehovot, Israel.

† Abbreviations: ϕX174 RF I, intact (un-nicked) circular duplex intracellular replicative form of bacteriophage ϕX174 DNA; ϕX174 RF II double-stranded relaxed circular DNA with at least one single strand break. SV40, simian virus 40.

Wang (1969) and Vinograd *et al.* (1968) have all noted that the number of superhelical turns apparent in electron micrographs is very different from that calculated from sedimentation-velocity–dye titration experiments for the same molecules. Possible reasons for this have been discussed by Vinograd *et al.* (1968) and Kleinschmidt *et al.* (1965).

The technique of light-scattering offers a means of obtaining a molecular weight, a root-mean-square radius and a simple light-interference pattern for these molecules (Geiduschek & Holtzer, 1958); these are direct measures of molecular conformation. We have previously reported that ϕX174 RF I DNA at $\sigma = -0.025$ (−12 superhelical turns) is best represented by a Y shape by using this technique (Campbell & Jolly, 1972; Jolly & Campbell, 1972*a*). It is obvious, however, that structure transitions must occur as the superhelix density alters in such molecules, since the variation of *s* value with superhelix density is itself multiphasic. We have therefore performed light-scattering experiments on ϕX174 RF I DNA at different superhelix densities. The superhelix density was altered by two methods which are reasonable characterized and controlled: (*a*) by temperature variation and (*b*) by drug intercalation. For the latter we chose to perform experiments in the presence of proflavine, which is known to intercalate and unwind superhelical DNA molecules with negative turns (Blake & Peacocke, 1968; Waring, 1970), and which does not absorb light at 546nm (except when concentrated) in aqueous solution. Proflavine has previously been used successfully in light-scattering experiments on DNA (Mauss *et al.*, 1967).

A preliminary report of some of these results has already been presented (Jolly & Campbell, 1972*b*).

Materials and Methods

Preparation and analysis of DNA

The replicative double-stranded form of ϕX174 DNA was prepared, and the two forms were separated as described previously (Jolly & Campbell, 1972*a*). All light-scattering experiments were performed under nuclease-free conditions with sterilized glassware. The DNA was analysed in a Spinco model E ultracentrifuge before and after the light-scattering experiments by band sedimentation. This is obviously of limited value when the supercoils are nearly titrated to open circles. However, from our previous work we were confident of being able to handle the DNA without introducing single-strand nicks and even the smallest concentrations of proflavine hemisulphate used in these experiments protected the DNA markedly against nicking.

Light-scattering measurements

All light-scattering measurements were performed in a Fica 50 photogoniodiffusometer as described before (Jolly & Campbell, 1972*a*) in BPES buffer (6mM-Na_2HPO_4, 2mM-NaH_2PO_4, 1mM-EDTA and 0.179M-NaCl, pH6.8). Unpolarized incident light at 546nm was used and the solutions were clarified with the usual procedures. No anisotropy and fluorescence were detectable.

In the temperature experiments temperature control was achieved with the system fitted to the instrument, whereby the benzene vat in which the sample cell sits is thermostatically controlled. Dilutions were made at room temperature and the solution heated up and cooled down in the scattering cell. Corrections taking into account the effect of temperature were made for the refractive index of the buffer and deviation of the temperature of the sample-cell contents from that of the benzene vat, after coming to equilibrium; this latter correction was necessary because the sample-cell holder is metal and in contact with the metal frame of the instrument, leading to heat conduction, so that at high temperatures the cell contents were at a slightly lower temperature than the benzene, e.g. 1°C less when the benzene was at 55°C.

In the experiments with proflavine the approximate desired value of *r*, the number of mol of dye bound/mol of nucleotide, was achieved by adjusting the buffer for dialysis to the corresponding free dye concentration, equilibrating the previously dye-free sample for 8h, exchanging the buffer, and dialysing for a further 48h at room temperature in the dark to achieve complete equilibrium. The dialysis tubing absorbed fairly large amounts of dye but this did not affect the experiment. The filters for clarification also absorbed large amounts of dye and had to be equilibrated first with at least 150ml of diffusate, and then, for the sample filter, several passages of the DNA solution. Even then there were sometimes small, unpredictable absorptions and desorptions of dye, so every scattering solution was analysed spectrophotometrically as described below for dye binding and DNA concentration.

Refractive-index increment

The value of the refractive-index increment used in the absence of dye was 0.166ml/g for DNA in BPES buffer. This does not change significantly with temperature (Krasna, 1970). The values at different values of *r* were obtained by using calf thymus DNA dialysed to equilibrium for more than 48h in BPES buffer with added proflavine hemisulphate. The experiments were performed in a Brice–Phoenix differential refractometer at 25±0.1°C with unpolarized light at 546nm. A range of four DNA concentrations (90–600μg/ml) was used to determine the refractive index increment, dn/dc (where n is the refractive index and c the DNA concentration), at $r = 0$, 0.098 and 0.102, whereas at intermediate

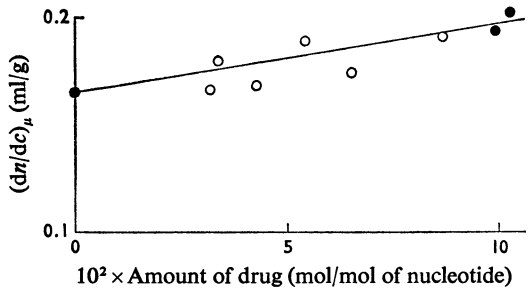

Fig. 1. *Refractive index increment of DNA at various values of bound proflavine*

$(dn/dc)_\mu$ is the refractive index increment at constant chemical potential, μ; the DNA used was calf thymus. ○, dn/dc from one concentration of DNA; ●, dn/dc from a range of four or five concentrations of DNA. The line is a weighted fit of the points (●:○ = 4:1) to a straight line by the least-squares method. The dn/dc values required for light-scattering experiments were read off this plot.

values of r single concentrations of DNA were used. This is shown in Fig. 1.

Titration of ϕX174 RF I DNA by ultracentrifugation with proflavine hemisulphate

This was performed by using boundary sedimentation with Kel-F centre-pieces at 25°±0.3°C in a Spinco model E analytical ultracentrifuge at 35600rev./min, taking photographs at 8min intervals and following the method of Waring (1970). The temperature control system was switched to 'indicate' after reaching speed to avoid convection disturbances (Studier, 1965) and thereafter during a run stayed almost constant. The sedimentation coefficients were not corrected for buoyancy to 20°C or extrapolated to zero concentration as they are all internally consistent.

Proflavine binding and DNA concentrations

Measurements of binding were made by using the formulation of Peacocke & Skerret (1956) and the method of Waring (1965, 1970). Measurements were made on three solutions at 440nm in 1cm-path-length cells in a water jacket thermostatically controlled to 25°±0.1°C: (*a*) BPES buffer, (*b*) calf thymus DNA at a concentration of 500μg/ml in BPES buffer, (*c*) ϕX174 RF I DNA, $E_{260} = 0.600$ in BPES buffer. The proflavine hemisulphate solution at 44.9μg/ml was added in the same proportions as the proflavine hemisulphate added to the bulk solution in the sedimentation experiment. Thus cell (*c*) mimics the conditions in the sedimentation cell, cell (*b*) gives absorbance if all the dye is bound, and cell (*a*) gives absorbance if all the dye is free. The dye bound to ϕX174 DNA can then be calculated as described in Peacocke & Skerret (1956). Proflavine binding to DNA was investigated by spectral examination of calf thymus DNA, proflavine hemisulphate and calf thymus DNA plus proflavine hemisulphate in the visible region by using a modification and extension of the method of Peacocke & Skerret (1956) and in the u.v. in BPES buffer at room temperature (20–23°C) in 1cm-path-length cells, except where otherwise specified. Previous binding experiments indicated no change in experiments conducted in this manner from those under strict temperature control at 25°C. The usual procedure was to set up cuvettes with 2.4ml of solution and add 20–50μl portions of stock proflavine hemisulphate solution, about 45μg/ml, or BPES buffer as required. The cuvettes were then sealed with Parafilm, mixed by several inversions and allowed to equilibrate for 5min. In fact, binding seemed to occur very rapidly and the first spectrum it was possible to obtain never altered after up to 2h equilibration. In all these experiments, proflavine hemisulphate concentrations were found by using the well-established value of $\epsilon = 4.1 \times 10^4$ litre·mol^{-1}·cm^{-1} for the free dye at the maximum at 443–444nm (Haugen & Melhuish, 1964; Gersch & Jordan, 1965; Blake & Peacocke, 1968; Cohen & Eisenberg, 1969). Spectra of free and bound proflavine (i.e. in a solution of DNA, approx. 1.8mmol of nucleotide/l) from 480nm to 400nm were run first at proflavine hemisulphate concentrations from 1.34 to 17.1μM; a DNA blank was used for the bound proflavine and some measurements at lower concentrations were made in 5cm-path-length cells.

In these experiments and all later ones an isobestic point was observed at 454±0.3nm, as noted first by Peacocke & Skerret (1956). The absorbances at 454nm were plotted against those at 440 and 460nm of bound and free dye and the best straight line found by the least-squares method. All four sets of points were extremely good straight lines with linear regression coefficients above 0.998, and the ratios E_{440}/E_{454} and E_{460}/E_{454} for bound and free dye found from the gradients. E_{444} was also plotted against E_{454} for the free dye and from this gradient $\epsilon_{454} = 3.398 \times 10^4$ litre·mol^{-1}·cm^{-1} was calculated from $\epsilon_{444} = 4.1 \times 10^4$ litre·mol^{-1}·cm^{-1}. Results of these analyses are included in Table 1. From one visible spectrum of DNA plus proflavine hemisulphate it was then possible to obtain the total proflavine hemisulphate concentration and the absorbances of totally bound and free dye of the same concentration at 440 and 460nm, from the absorbance at 454nm. This, together with the actual absorbances at 440 and 460nm, allows the use of the method of Peacocke & Skerret (1956) to determine the amount of dye bound from

Table 1. *Relative proflavine extinction coefficients from spectral analyses*

Results of the spectral ratios plotted as described in the Materials and Methods section are given. The values in the first two columns are the wavelengths of light in nm at which the absorbances have been plotted on that particular axis, and b and f indicate bound and free proflavine respectively. The final column gives the calculated molar extinction coefficients at the wavelengths and conditions defined in the *y*-axis column. The bottom line refers to the plot to determine the extinction coefficient of bound proflavine at 260nm; D_f, D and c_b are the absorbance if all the dye is free, the absorbance of bound and free dye, and the concentration of bound dye, respectively.

y axis	*x* axis	Gradient	Regression coefficient	$10^{-4} \times \epsilon$ (litre·mol^{-1}·cm^{-1})
454	444f	0.8287	0.9984	3.398
440f	454	1.1947	0.9984	4.060
460f	454	0.7668	0.9988	2.606
440b	454	0.7129	0.9980	2.422
460b	454	1.0401	0.9983	3.534
225.5	444f	0.3201	0.9999	1.312
260f	444f	1.3641	1.0000	5.593
$10^2 \times (D_f - D)$	c_b (μM)	2.4450	0.9991	3.143

readings at 440 and 460nm. Peacocke & Skerret (1956) found that the specific absorbance of bound proflavine at 460nm varied with *r*, the amount of dye bound (mol/nucleotide pair). As witnessed by the linearity of the absorbance-value plots this has not been observed; neither do binding results calculated from absorbances at 460nm in later experiments differ in a significant manner from results from 440nm, although the error of the former is somewhat larger. However, Peacocke & Skerret (1956) were working to a large extent at values of *r* above those in the present investigation, and Blake & Peacocke (1968) have since found that the variation at 460nm could be attributable to experimental error.

Further spectra from 480 to 400nm and 300 to 220nm were run for proflavine hemisulphate alone, in the presence of moderate DNA concentrations (approx. 0.1 and 0.13mmol of nucleotide/l) and the same DNA solutions without dye. A further isobestic point at 225.5nm was found, as reported by Cohen & Eisenberg (1969). Plotting $E_{225.5}$ against E_{444} for free dye gave a straight line and $\epsilon_{225.5}$ of 1.312×10^4 litre·mol^{-1}·cm^{-1} for proflavine. Thus for any DNA plus proflavine hemisulphate solution within certain limits, the absorbances at 460, 454, 440 and 225.5nm lead to accurate values of bound dye, DNA concentration and hence *r*. The value of $\epsilon_{P,225.5}$ for the calf thymus DNA used in all these experiments and in differential refractometry was 3101 ($\epsilon_{P,260}$ = 6541) from spectral analysis by the method of Hirschman & Felsenfeld (1966). DNA concentrations and *r* values in the refractive index increment experiments were determined this way.

However, in the light-scattering experiments a u.v.-absorbing contaminant in the membrane filters, which has been previously noted (Dawson & Harpst, 1971), make readings in the far u.v. at 225.5nm unreliable despite thorough prerinsing of the filters. However, at least as far as 240nm, readings are always completely unaffected, if prerinsing is thorough, and for light-scattering samples concentrations were determined by E_{260}. It was, therefore, necessary to determine E_{260} of bound and free proflavine, from the previous results. For the free dye, absorbances at 444 and 260nm were plotted as usual, giving $\epsilon_{260} = 5.593 \times 10^4$ litre·mol^{-1}·cm^{-1}. For bound dye, the concentration, c_b, was found from the visible spectra; then from $(D_f - D) = c_b(\epsilon_f - \epsilon_b)$, where D_f is the absorbance if all the dye is free, D is the absorbance of bound and free dye (DNA absorbance subtracted) and ϵ_f and ϵ_b are the free and bound dye extinction coefficients respectively, a plot of $(D_f - D)$ against c_b should give a straight line, gradient $(\epsilon_f - \epsilon_b)$. This is the case and $\epsilon_b = 3.143 \times 10^4$ litre·mol^{-1}·cm^{-1} at 260nm. Thus knowing the concentration of bound and free dye from the visible spectrum and the extinction coefficient at 260nm an absorbance at 260nm is obtained for the DNA, which is readily convertible into concentration.

It was desirable to check the accuracy of these two methods of DNA concentration measurement and this was done by examining five solutions of calf thymus DNA (0.101mmol of nucleotide/l) at different total proflavine hemisulphate concentrations (3–12μM). By both methods, the known DNA concentration was refound to within 0.5%.

Table 1 shows the extinction coefficients etc.

Analysis of data

The experimental data were processed and the theoretical light-scattering curves calculated on a PDP 8/L digital computer.

Results

Temperature experiment

Experiments were performed at ten temperatures from 14.9°C to 74.5°C. The results were interpreted as usual by means of Zimm (1948) plots; in all cases the concentration ranges were approx. 30–80 μg/ml except at 74.5°C where it was 40–180 μg/ml. In all experiments the molecular weight was in the range $3.2\times10^6\pm0.12\times10^6$, in agreement with previous results (Jolly & Campbell, 1972*a*,*c*). The results for the root-mean-square radii, second virial coefficients and temperatures at which experiments were performed are given in Table 2, typical Zimm plots are shown in Fig. 2, the resulting reciprocal particle-scattering factor, $P(\theta)^{-1}$, curves in Fig. 3 and a plot of root-mean-square radius against temperature in Fig. 4.

The dependence of superhelix density on temperature has been investigated by Wang (1969) and Upholt *et al.* (1971). Because of the insensitivity of sedimentation coefficient to superhelix density between $|\sigma| = 0.036$–0.016, approximate estimates for the temperature coefficient ($\Delta\sigma$/°C) have been made only above and below these values. Upholt *et al.* (1971) found $\Delta\sigma/°C = 1.5\times10^{-4}$ above, and 1.6×10^{-4} below these values of σ for SV 40 DNA and Wang (1969) found $\Delta\sigma/°C = 1.4\times10^{-4}$ at values of σ above 0.036. Hence a value of 1.5×10^{-4} was used for ϕX174 RF I DNA for $|\sigma| = 0.027$–0.017. This means that it is assumed that one full superhelical turn is lost for a rise in temperature of about 13°C. However, these coefficients were determined from 0° to 40°C and, although σ appears to change with temperature close to linearly within this range, the extrapolation of the data of these authors to 74.5°C remains open to further experimental proof and may not be entirely valid as the DNA is undergoing a major structural transition in this range. Any doubt would centre on the highest temperature where it would be conceivable that early melting may occur. Vinograd *et al.* (1968) estimated the T_m ('melting' temperature) o polyoma I DNA, which has a G-C content of 48% (ϕX174 RF DNA has one of 42%), as 108°C in a buffer equivalent to BPES buffer; in addition they estimated a T_m of 77°C for the early melting, which seems to occur in the A-T-richest section of the duplex owing to the destabilizing effect of superhelical turns. In such a situation the change of σ with temperature might well deviate from linearity. However, all these experiments are performed well below the T_m for melting and below the T_m for early melting. Also the results obtained by unwinding with proflavine hemisulphate are qualitatively similar in this region (see below) and any effect is probably therefore small.

It can be seen that although there are some apparent small variations in the root-mean-square radius from $\sigma = -0.0265$ (−13 superhelical turns, 14.9°C) to $\sigma = -0.0207$ (−10 superhelical turns, 53.4°C), a major transition in solution structure occurs between $\sigma = -0.0207$ and $\sigma = -0.176$ (−8 superhelical turns, 74.5°C). This is borne out by the change in the $P(\theta)^{-1}$ plots (Fig. 3). In this region of superhelix density the sedimentation coefficient appears to be insensitive to structural changes and shows a very slight increase from its value at −12 superhelical turns. Presumably the molecule has become less free-draining (Tanford, 1961) although more compact as it unwinds from −10 to −9 superhelical turns. The actual conformation of this compact structure at $\sigma = -0.0176$ is interesting and three possible structures are shown in Fig. 5; (*a*) and (*b*) are variations

Table 2. *Dependence of molecular parameters of ϕX174 RF I DNA on temperature*

The root-mean-square radius, *Rg*, and second virial coefficient, *B*, were obtained from the light-scattering experiments described in the text at the indicated temperatures. Correlation of the superhelix density, σ, and superhelical winding number, τ, with temperature change was made by using a temperature coefficient of $\Delta\sigma/°C = 1.5\times10^{-4}$, chosen as described in the text.

Temperature (°C)	*Rg* (nm)	$10^5\times B$ (mol·cm^3·g^{-2})	$10^2\times-\sigma$	$-\tau$
14.9	85.4±11	7.15±4	2.65	12.5
20.3	85.3±11	6.76±4	2.57	12.1
25.4	92.0±12	−8.57±5	2.50	11.8
30.3	92.8±12	1.47±1.5	2.42	11.4
35.4	93.2±12	2.06±2	2.34	11.0
39.8	92.5±12	3.05±3	2.28	10.8
45.0	95.2±12	4.14±3	2.20	10.4
49.5	88.0±11	8.24±5	2.15	10.1
53.4	83.2±11	1.47±1.5	2.07	9.8
74.5	62.0± 9	2.0 ±2	1.76	8.3

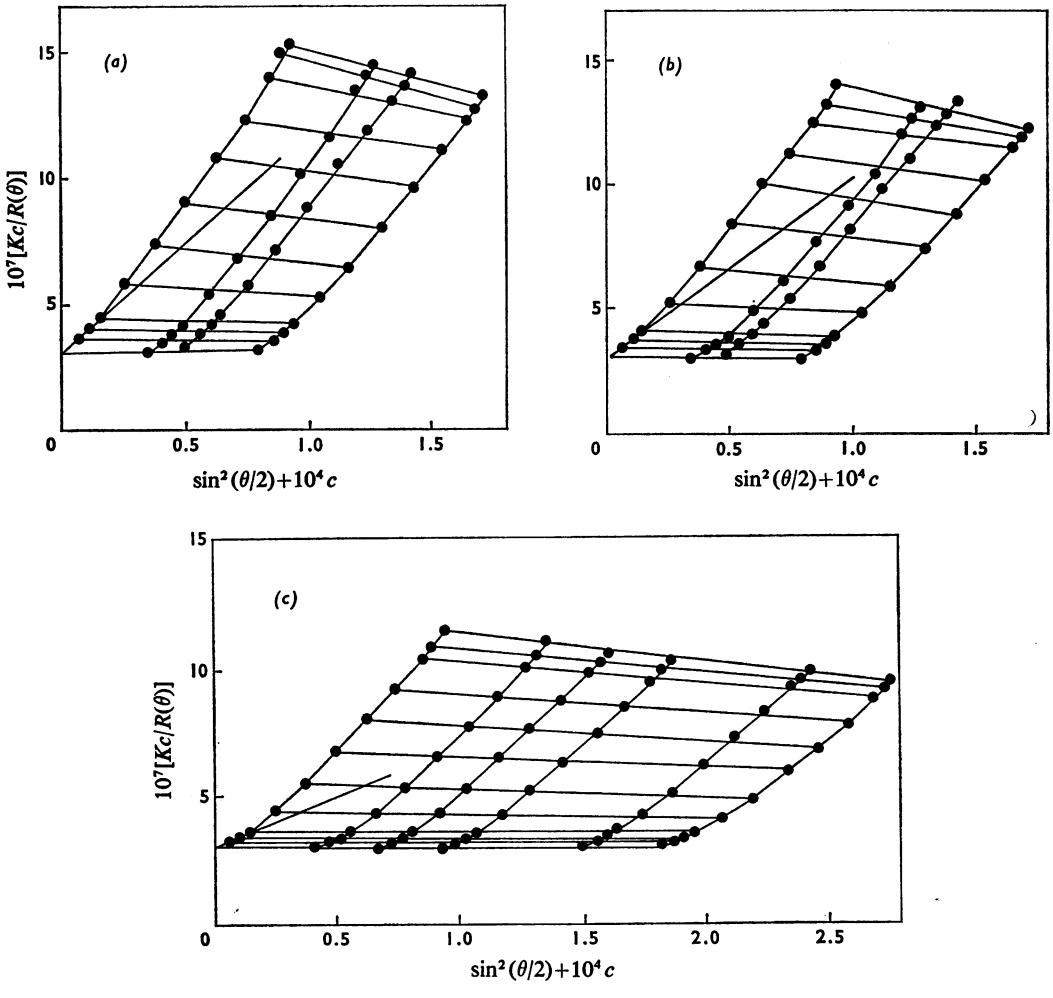

Fig. 2. *Zimm plots of experiments on $\phi X174$ RF I DNA at temperatures from 45°C to 74.5°C*

(*a*) 45.0°C, (*b*) 53.4°C, (*c*) 74.5°C. The scattering angle, θ, varied from 30° to 150° and all units are in the c.g.s. system. The formula $[Kc/R(\theta)]_{\theta=0} = 1/M$ allows the estimation of the molecular weight, M, where $K = 2\pi^2 n^2 (dn/dc)^2/N\lambda^4$ is a constant in any one experiment and $R(\theta) = r^2 i_\theta / I_0(1+\cos^2\theta)$. Here n is the refractive index of the solvent, dn/dc the refractive index increment, N Avogadro's number, λ the wavelength of light *in vacuo*, c is the concentration in g/ml, i_θ the intensity of scattered light at θ, I_0 the intensity of incident light, both per unit volume, and r is the distance of the receiver from the scattering point. The formula $[Kc/R(\theta)]_{c=0} = (1/M)[1/P(\theta)] = (1/M)[1+16\pi^2 Rg^2 \sin^2(\theta/2)/3(\lambda/n)^2+\cdots]$ allows estimation of the root-mean-square radius, Rg, from the initial slope of $Kc/R(\theta)$ at zero concentration, and the particle-scattering factor, $P(\theta)$, which is 1 at 0°. $P(\theta)$ = (scattered intensity at θ)/(scattered intensity at 0°) = $[Kc/R(\theta)]_{\theta=0}/[Kc/R(\theta)]_{c=0}$. The formula $[Kc/R(\theta)]_{\theta=0} = 1/M+2Bc+\cdots$ allows estimation of the second virial coefficient, B.

of the straight interwound and toroidal models, and (*c*), which is related to (*b*), has been considered by Glaubiger & Hearst (1967). The mathematical derivations of the various models are presented in the Appendix. The experimental results together with theoretical curves for the two models are shown in Fig. 6. The experimental results fall just outside the maximum error curve for the toroid model and well outside that for the straight interwound model. Thus no hard conclusion can be drawn from these experiments alone although some toroid-like structure is suggested.

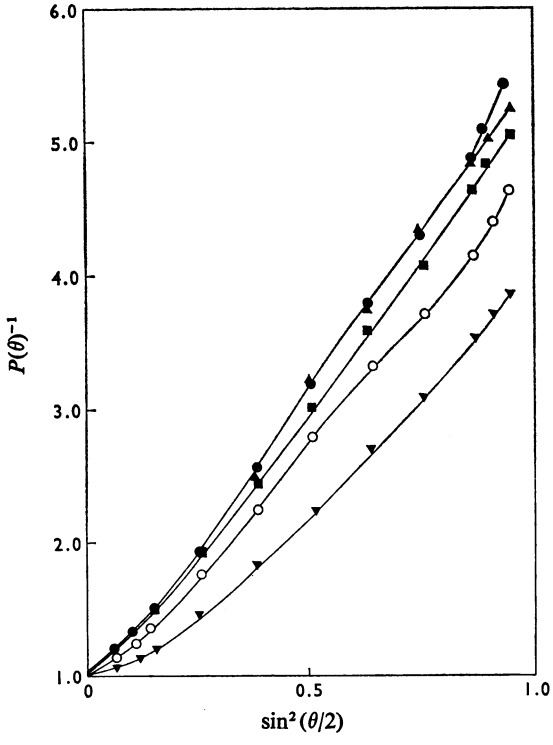

Fig. 3. *Variation of the curves of* $P(\theta)^{-1}$ *against* $\sin^2(\theta/2)$ *with temperature for* $\phi X174$ *RF I DNA*

The curves at temperatures intermediate to those for which curves are shown, were intermediate in position. Details of results at these and the other temperatures are given in Table 2. ●, 25.4°C; ▲, 14.9°C; ■, 45.0°C; ○, 53.4°C; ▼, 74.5°C.

At first inspection it would appear that these data disagree with the data of Follet & Crawford (1967) and Rhoades & Thomas (1968) who have shown that the supercoil is completely unwound to a circle by 50°C and at higher temperatures takes on positive superhelical turns. However, these authors used the technique of formaldehyde fixing at various temperatures and then analysed the DNA structure at room temperature by using sedimentation or electron microscopy. This is obviously not directly comparable with results obtained by a study performed at the elevated temperatures themselves. Although it is possible to suggest that the different buffer conditions used by these authors is responsible for the discrepancy, it seems more likely that formaldehyde fixing reflects the continuing dynamic structure of the DNA (Utiyama & Doty, 1971), i.e. the transient breaking and joining of the hydrogen bonds, whereas light-scattering reflects the statistical average of these at any moment in time.

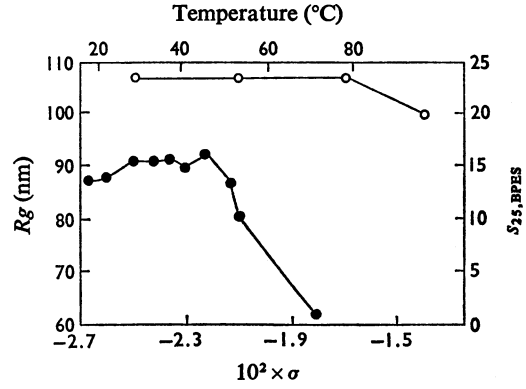

Fig. 4. *Variation of the root-mean-square radius of* $\phi X174$ *RF I DNA with temperature and superhelix density*

Results are translated into a dependence on superhelix density (σ) as described in the text; the maximum errors are shown in Table 2. Also shown, for reference, are results from an ethidium bromide titration converted into dependence on superhelix density. ●, Root-mean-square radius (Rg); ○, sedimentation coefficient ($s_{25,BPES}$).

Proflavine experiments

Binding of proflavine to $\phi X174$ *RF I.* The binding curve found with the solutions from light-scattering experiments is shown in Fig. 7. There are no previous curves published for proflavine binding to supercoiled DNA, but the curve seems qualitatively compatible with binding curves for linear DNA (Peacocke & Skerret, 1956; Cohen & Eisenberg, 1969) taking into account the higher initial affinity of supercoiled DNA for intercalating ligands (Bauer & Vinograd, 1968, 1970).

Sedimentation-coefficient dependence on dye binding. The values are plotted in Fig. 8. The minimum is assumed to be the point where the open circular conformation is achieved. The critical binding ratio at this point, r_c, is 0.061 ± 0.003 mol of dye/mol equiv. of nucleotide. Assuming that both the value of the number of superhelical turns, τ, $= -11.8 \pm 1.6$ (Jolly & Campbell, 1972*a*) from ethidium bromide titration and an unwinding angle of 12° in the DNA helix per ethidium bromide molecule bound are correct, this gives an apparent unwinding angle of $7.3° \pm 1.3°$ per bound proflavine molecule, in good agreement with the values of 8° and $8.4° \pm 2.4°$ found by Saucier *et al.* (1971) and Waring (1970) respectively, and a value of 7.3° was used in the estimation of σ for the light-scattering experiments. Thus an increment of 0.005 mol of dye/mol equiv. of nucleotide in r results in the loss of one superhelical

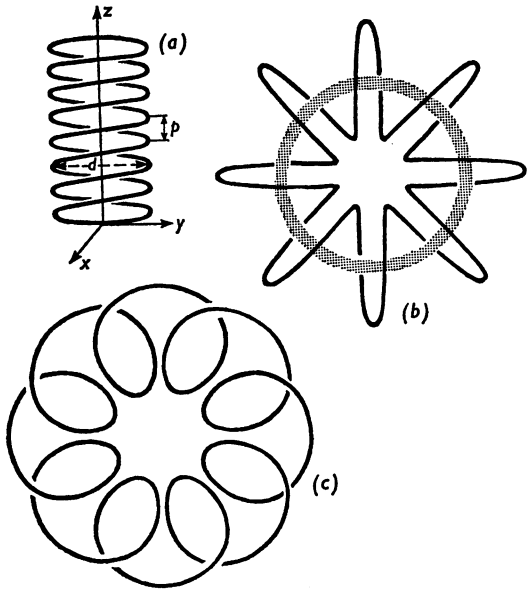

Fig. 5. *Hypothetical structures for various of supercoiled $\phi X174$ RF I DNA with eight superhelical turns*

The solid line represents the DNA duplex. (*a*) Straight interwound model with large superhelix radius of the same order of dimensions as the length; *d* is the superhelix diameter and *p* the pitch (see the Appendix). (*b*) Toroidal model with small and large radii of similar size. (*c*) Flattened toroidal model; this is related to structure (*b*), and has been considered by Glaubiger & Hearst (1967).

turn ($\Delta\sigma = 0.002$). The curve is biphasic, as was the ethidium bromide titration curve, with the maximum occurring at $r = 0.0208$ mol of dye/mol equiv. of nucleotide, $\sigma = -0.017$, which coincides with that from the ethidium bromide titration. There is a possibility that not all the bound dye intercalates (Ramstein *et al.*, 1972) and the real unwinding angle per intercalating molecule is larger, but at the amounts of dye used here this seems unlikely, and has no effect on the results of the experiments.

Light-scattering. Zimm (1948) plots of results obtained at two values of *r*, 0.017 and 0.024 mol of dye/mol equiv. of nucleotide, are shown in Fig. 9. Zimm (1948) and Berry (1966) plots of results at $\sigma = -0.0004$ are shown in Fig. 10. The Berry (1966) plot is useful for extending the range of molecular dimensions, which can be examined by light-scattering, down to 30° by eliminating some of the curvature at low angles semi-empirically by plotting $[Kc/R(\theta)]^{\frac{1}{2}}$, not $Kc/R(\theta)$, on the ordinate. No anisotropy was detectable from the zero value of the

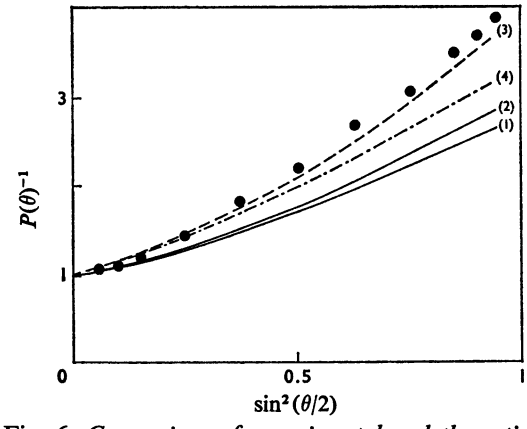

Fig. 6. *Comparison of experimental and theoretical $P(\theta)^{-1}$ curves for the compact structure formed by $\phi X174$ RF I DNA at 74.5°C*

The points indicate the experimental results, the lines computer-calculated curves for theoretical models. Curve (1), toroidal model, root-mean-square radius (Rg) = 62 nm, number of superhelical turns (τ) = 8. With this model, $d = 63.8$ nm and $p = 45.4$ nm. Curve (2), interwound model, $Rg = 62$ nm, $\tau = 8$. With this model, the large radius is 53.1 nm and the small radius 32.0 nm. Curve (3), toroidal model upper maximum error data, $Rg = 71$ nm, $\tau = 10$. Curve (4), interwound model upper maximum error data, $Rg = 71$ nm, $\tau = 10$.

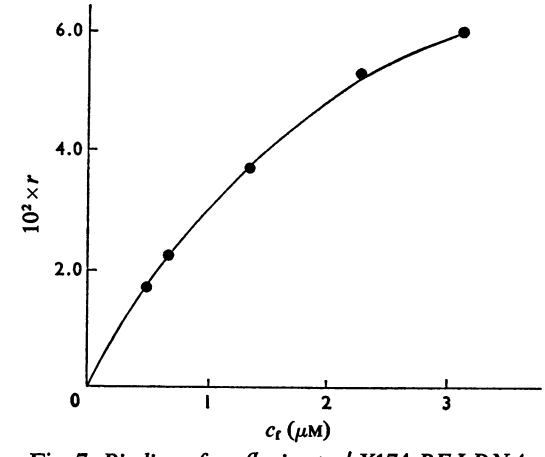

Fig. 7. *Binding of proflavine to $\phi X174$ RF I DNA*

c_f is the concentration of free dye and *r* is the amount of dye bound (mol/mol equiv. of nucleotide). The results are from the solution used for light-scattering and each point represents the mean of results from the solutions of one complete light-scattering experiment. Hence the DNA concentration was 20–50 μg/ml. The solvent was BPES buffer and the temperature 20–23°C.

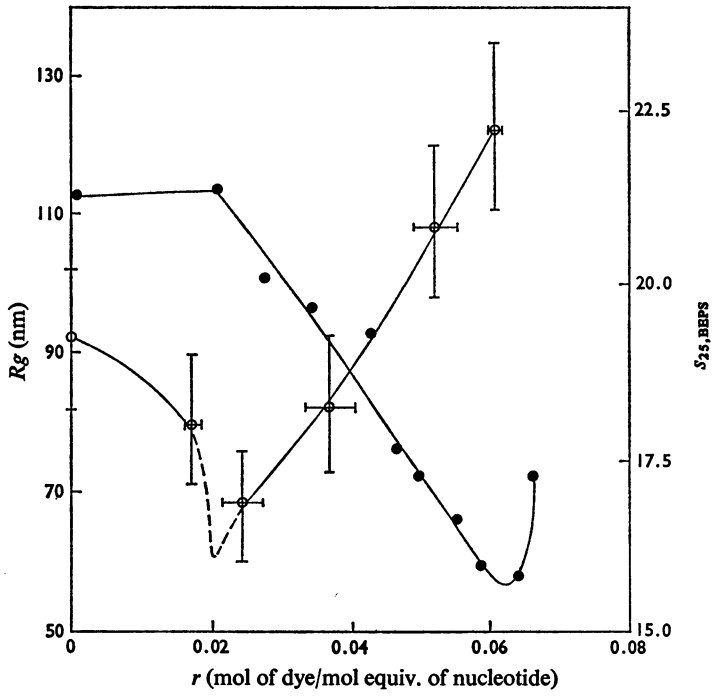

Fig. 8. *Sedimentation coefficient and root-mean-square radius of $\phi X174$ RF I DNA as functions of the binding of proflavine*

All experiments were done at 25°C. Sedimentation coefficients ($s_{25,BEPS}$; ●) were not corrected to standard conditions. The errors in the root-mean-square radius (vertical bars) were estimated by least-good initial slopes in the Zimm and Berry plots; the errors for r (horizontal bars) represent the variation in r for samples used in the same Zimm or Berry plot to estimate the root-mean-square radius (Rg; ○); any other errors are negligible compared with this. The dashed portion of the curve for the root-mean-square radius is hypothetical and based on the values obtained in the temperature titration.

horizontally polarized light component at a scattering angle of 90° extrapolated to zero concentration. Molecular weights for the four lower r values were all, after subtraction of bound proflavine, in the range $3.2\times10^6\pm0.05\times10^6$. For $\sigma=-0.0004$ the Zimm plot gave a molecular weight of 3.32×10^6, whereas the Berry plot gave 3.15×10^6, thus justifying its use. These values are in excellent agreement with our previous results (Jolly & Campbell, 1972*a*,*c*). The results for the root-mean-square radius, Rg, and second virial coefficient, B, as functions of r and σ are shown in Table 3. The Rg values are plotted as a function of r on the same diagram as the sedimentation-coefficient plot against r in Fig. 8. A sharp decrease in Rg at around $\sigma=-0.017$ is evident, before an increase to a value corresponding to an open circle at $\sigma=-0.0004$. The curves of $P(\theta)^{-1}$ in Fig. 11 also indicate these trends in conformation transitions; the curve for $\sigma=-0.0004$ was constructed by using the intercept from the Berry plot at zero angle, and the extrapolation to zero concentration at finite angles from the Zimm plot.

Fit of experimental results to the theoretical models. The $P(\theta)^{-1}$ curves at $\sigma=-0.018$ (−9 superhelical turns) and −0.015 (−8 superhelical turns) were compared with the same two types of models, the straight interwound model with large radius and the compact toroid, as considered for the compact structure above in the temperature experiments. It was assumed that each bound dye molecule extended the DNA length by 0.335nm (Drummond *et al.*, 1966). These results are shown in Fig. 12. At $\sigma=-0.018$, the experimental results fall well within the error range for the toroid model and well outside that for the interwound model. At $\sigma=-0.015$ the experimental results fall outside the error ranges of both models but nearer the toroid limit, reminiscent of the situation in the temperature experiment.

For $\sigma=-0.018$, the dimensions of the models from experimental results were: toroid model, large radius

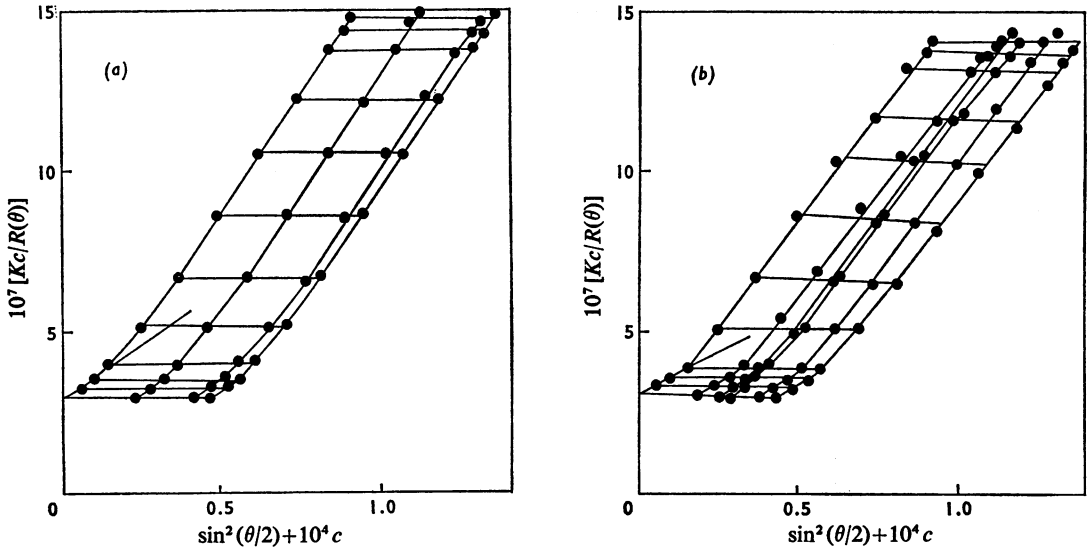

Fig. 9. *Zimm plots of ϕX174 RF I DNA at different values of bound proflavine*

All units are in the c.g.s. system, and the values of r (mol of bound dye/mol equiv. of nucleotide) are indicated. The scattering angle, θ, was 150°–30°, DNA concentrations were approx. 20–45 μg/ml and the temperature was 25°±0.2°C. For further details see the legend to Fig. 2. In (*a*), $r = 0.017$, $\sigma = -0.0178$; and in (*b*) $r = 0.024$ and $\sigma = -0.0154$.

74.2nm, small radius 28.9nm; straight interwound model, superhelix diameter 57.4nm, pitch 56.1nm. For $\sigma = -0.015$ the dimensions were: toroid model, large radius 56.8nm, small radius 38.3nm; straight interwound model, diameter 76.4nm, pitch 54.3nm. It seems, therefore, that at $\sigma = -0.018$ the rigid toroid is a reasonable model for the molecule, but at $\sigma = -0.015$ this model breaks down somewhat.

At $\sigma = -0.0004$ the molecule is almost exactly equivalent to RF II DNA, i.e. it is in an open circular form. Since there was a theoretical $P(\theta)$ function available for open circular DNA (Jolly & Campbell, 1972*c*), it was possible to use it to obtain $P(\theta)^{-1}$ curves for different persistence lengths (Kratky & Porod, 1949; Geiduschek & Holtzer, 1958; Flory, 1969). This was done, again assuming an extension of 0.335nm per bound dye molecule for the DNA thread, and the experimental results and theoretical curves are shown in Fig. 13. The persistence length of the DNA in this situation is estimated as 36.0±3.0nm from this plot.

Discussion

Molecular-weight values

One of the major difficulties encountered in interpretation of light-scattering experiments on nucleic acids has been extrapolation to zero angle (Schmid *et al.*, 1971). However, with ϕX174 RF DNA, due to its relatively small molecular mass and its compact circular conformation, this difficulty is not encountered. Thus at high superhelix densities extrapolation is from at least three points and from values of $P(\theta)^{-1}$ below 1.3, the approximate maximum limiting value for safe extrapolation to zero angle stipulated by Zimm (1948) and Schmid *et al.* (1971). At the highest dye concentration the DNA molecule is at its most extended and the above conditions are somewhat violated in the Zimm plot where some low-angle curvature is apparent. However, when the Berry (1966) plot is used this curvature is effectively eliminated and extrapolation is made from three points and $P(\theta)^{-\frac{1}{2}}$ of 1.3. It is relevant to note here that from these and other investigations (Jolly & Campbell, 1972*a*,*c*) the molecular weight of ϕX174 RF DNA may be estimated as $3.22\times10^6\pm0.05\times10^6$ (S.D. of 20 experiments). This downward re-evaluation of the molecular weight from the accepted value of 3.4×10^6 (Sinsheimer, 1959), which is suspect anyway (Schmid & Hearst, 1969), is in line with the recent small downward re-evaluation of the molecular weights of DNA molecules from the commonly used coliphages such as T4, T5, T7 and λ (Freifelder, 1970).

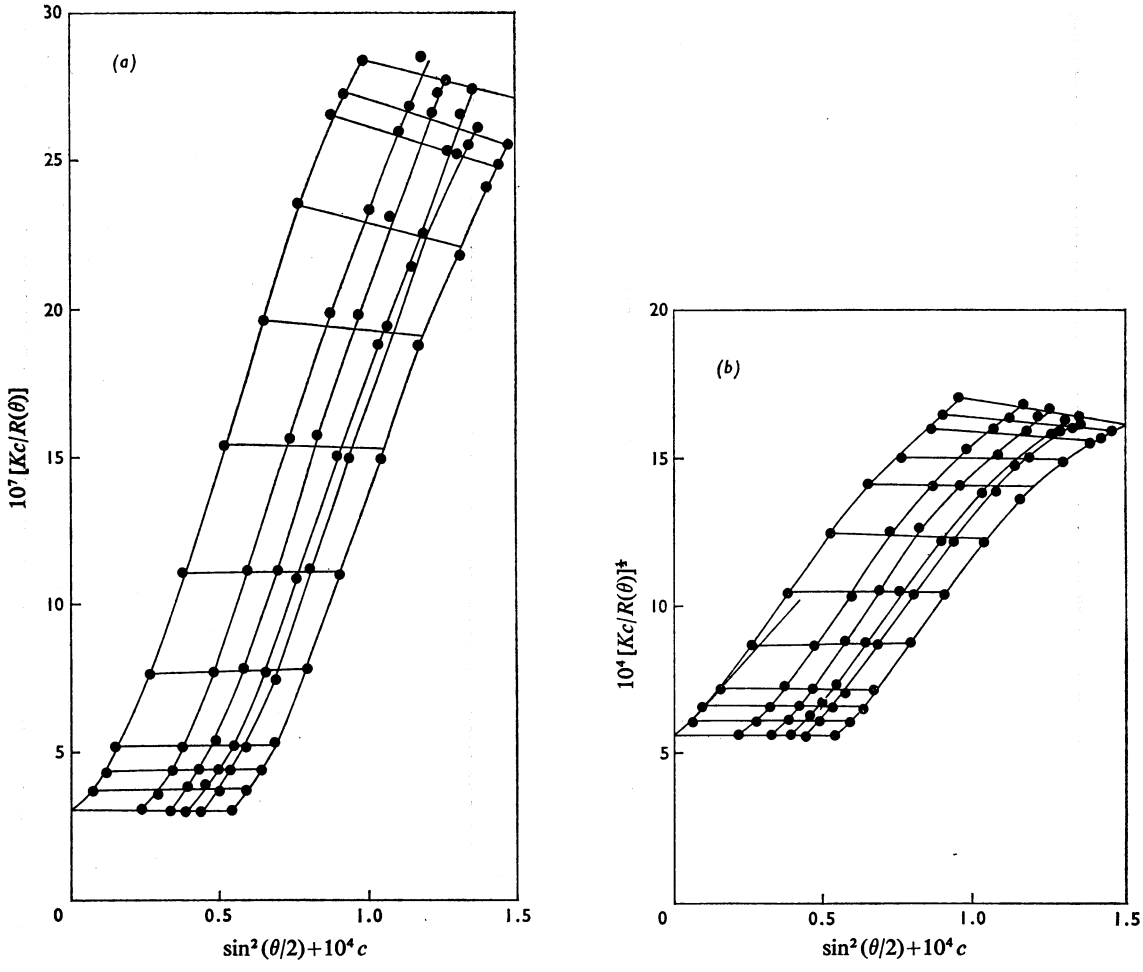

Fig. 10. *Zimm and Berry plots of $\phi X174$ RF I DNA with 0.06 mol of dye bound/mol equiv. of nucleotide*

The scattering angle was 150°–30°, the concentration range 20–50 μg/ml, the temperature 25°±0.2°C and all units are in the c.g.s. system. (*a*) Zimm plot. (*b*) Berry plot of the same data as in the Zimm plot. The formula $\{[Kc/R(\theta)]^{\frac{1}{2}}\}_{\theta=0} = 1/M^{\frac{1}{2}}$ gives the molecular weight. $\{[Kc/R(\theta)]^{\frac{1}{2}}\}_{c=0} = (1/M)^{\frac{1}{2}}[1/P(\theta)]^{\frac{1}{2}} = (1/M)^{\frac{1}{2}}(1+8\pi^2 Rg^2 \sin^2(\theta/2)/3(\lambda/n)^2+\cdots)$ gives Rg and $[Kc/R(\theta)]^{\frac{1}{2}}_{\theta=0} = (1/M+2Bc+\cdots)^{\frac{1}{2}} = (1/M)^{\frac{1}{2}}+BM^{\frac{1}{2}}c+\cdots$ allows estimation of B. $P(\theta) = \{[Kc/R(\theta)]^{\frac{1}{2}}\}^2_{\theta=0}/[Kc/R(\theta)]_{c=0}$ gives the values of the particle-scattering factor; the numerator is from the Berry plot, the denominator from the Zimm plot.

Table 3. *Dependence of molecular parameters of $\phi X174$ RF I DNA on the bound proflavine/nucleotide ratio*

Results of analyses of the Zimm and Berry plots (Figs. 9 and 10) at the various values of r are given.

$-\tau$	r (mol of dye/mol equiv. of nucleotide)	$10^2\times-\sigma$	Rg (nm)	$10^5\times B$ (mol·cm^3·g^{-2})
11.8	0	2.5	92.0±12	−8.57±5
8.5	0.017	1.80	79.6±10	−2.94±3.0
7.2	0.024	1.53	68.5± 9	−4.17±3.9
4.6	0.037	0.97	82.9±11	−2.94±3.0
1.7	0.052	0.36	109.0±13	0 ±3.0
0.2	0.060	0.04	119.9±15	0 ±2.0

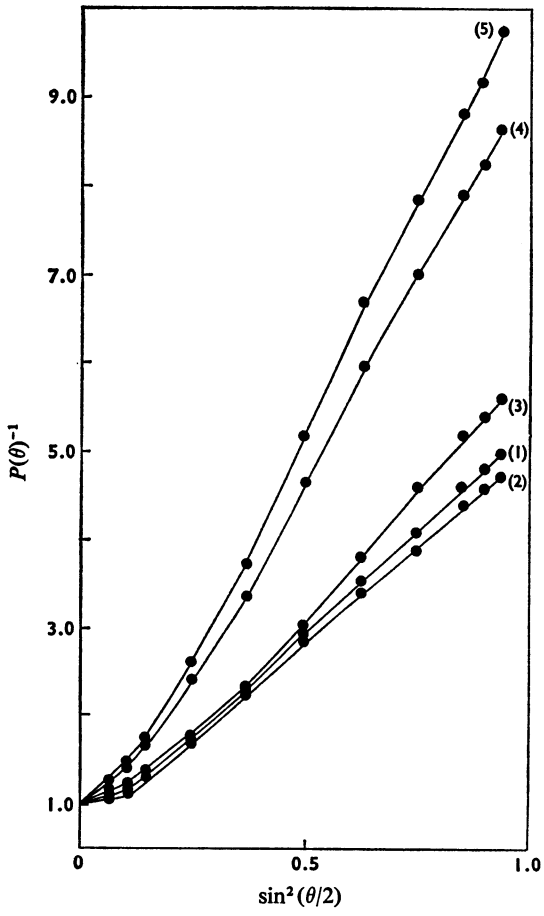

Fig. 11. *Reciprocal particle-scattering factors for $\phi X174$ RF I DNA at different amounts of dye bound (mol/mol equiv. of nucleotide)*

The curves were constructed from the respective Zimm and Berry plots as detailed in the legends to Figs. 9 and 10. The values of σ at which the curves were obtained were: (1) 0.0178 (−9 superhelical turns); (2) 0.0153 (−7 superhelical turns); (3) 0.0102 (−5 superhelical turns); (4) 0.0042 (−2 superhelical turns); (5) 0.001 (−0.5 superhelical turns).

Second virial coefficient

The second virial coefficient, B, is a measure of the deviation of the solution from ideality and theta conditions (Flory, 1953) when $B = 0$. The non-zero values of B found (Tables 2 and 3) are only just significantly different from zero but some qualitative comments are possible. As previously (Jolly & Campbell, 1972*a*) a small negative value of B was found at 25°C. If as previously suggested this is due

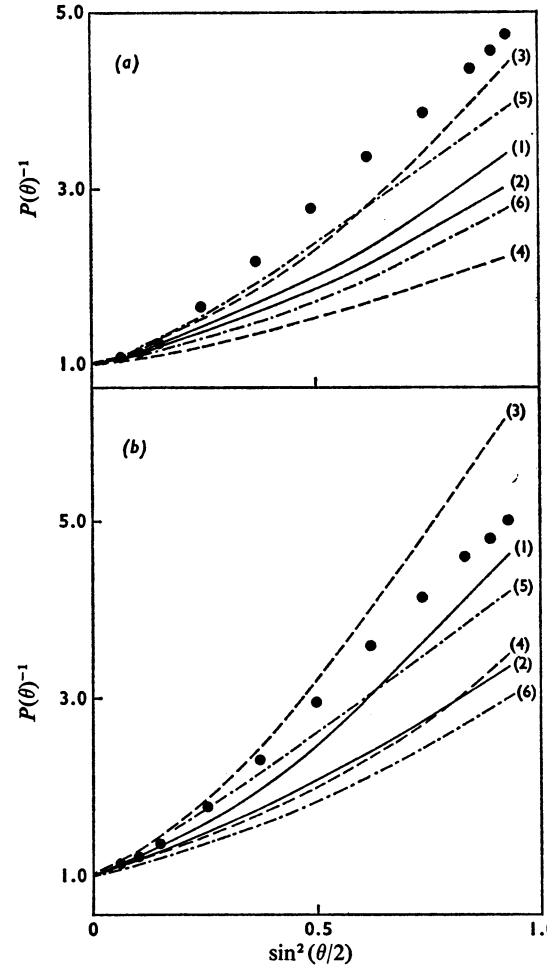

Fig. 12. *Comparison of experimental and theoretical $P(\theta)^{-1}$ functions for the compact supercoil conformations*

The points indicate the experimental results, the lines computer-calculated curves for theoretical models. (*a*) $r = 0.024$ mol of dye bound/mol equiv. of nucleotide, $\sigma = -0.0153$; curve (1), interwound model, $Rg = 68.5$ nm, number of superhelical turns (τ) = −7; curve (2), toroid model, $Rg = 68.5$ nm, $\tau = -7$; curves (5) and (6), interwound model maximum error data, $Rg = 78$ and 50 nm, $\tau = -8$ and −6 respectively; curves (3) and (4), toroid model maximum error data, $Rg = 78$ and 59 nm, $\tau = -8$ and −6 respectively. (*b*) $r = 0.017$ mol of dye bound/mol equiv. of nucleotide, $\sigma = -0.0180$; curve (1), toroid model, $Rg = 79.6$ nm, $\tau = -9$; curve (2), interwound model, $Rg = 79.6$ nm, $\tau = -9$; curves (3) and (4), toroid model maximum error data, $Rg = 89.5$ and 70 nm, $\tau = -10$ and −8 respectively; curves (5) and (6), interwound model maximum error data, $Rg = 89.5$ and 70 nm, $\tau = -10$ and −8 respectively.

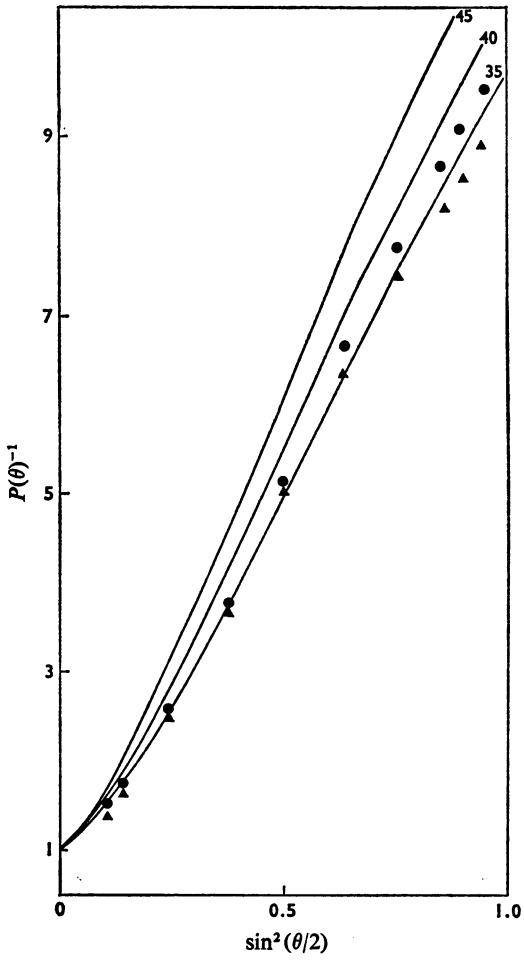

Fig. 13. *Comparison of experimental and theoretical $P(\theta)^{-1}$ curves for $\phi X174$ RF I DNA titrated to an open circle with proflavine*

●, RF I DNA with 0.06mol of dye bound/mol equiv. of nucleotide, that is virtually zero; ▲, RF II DNA, no dye present (Jolly & Campbell, 1972*c*). The lines are calculated for a theoretical $P(\theta)^{-1}$ function for a circular worm-like coil (Jolly & Campbell, 1972*c*). The values on the lines indicate the value of the persistence length used in nm; the points for RF I DNA are above those for RF II DNA, due, presumably, to extension of the duplex by intercalation.

to some small exposure of the hydrophobic interior of the double helix to solvent caused by torsional strain in the superhelix then it is to be expected that the value of B will tend to zero as the supertwists come out. ϕX174 RF II DNA is known to have a zero value of B (Jolly & Campbell, 1972*c*). This is indeed what happens as the molecule is unwound with proflavine. However, the variation of B with temperature clearly reflects a more complex situation. The appearance of positive values of B above and below 25°C is analogous to the behaviour of B for single-stranded poly(A) (Eisenberg & Felsenfeld, 1967), which at higher salt concentrations can actually be made to precipitate at about 25°C, although it dissolves above and below this. This effect may be attributed to the independent temperature variations of the enthalpy and entropy contributions to the free energy of solution of apolar bases in aqueous solutions (Sinanoglu & Abdulnur, 1964). At $\sigma = -0.025$ (−12 superhelical turns) the free energy of supercoiling is 78kcal/mol of DNA (see below) so that the free energy required to break a hydrogen bond is small in comparison (4kcal/mol) and the hypothesis that some hydrogen bonds are ruptured in the superhelix seems tenable. At high temperatures the virtual disappearance of B can be attributed to the decreasing torsional strain in the superhelix.

Shape changes

Qualitatively the results of unwinding by the two techniques seem to be in broad agreement and a schematic diagram of the transitions is shown in Fig. 14. From σ = approx. −0.027 to −0.021 (−13 to −10 superhelical turns) there are only small variations in the values of the root-mean-square radius and in the shape of the $P(\theta)^{-1}$ curves. However, when more of the molecule is unwound there is a sharp transition between $\sigma = -0.021$ and $\sigma = -0.017$ (−10 and −8 superhelical turns), the radius of gyration drops from above 90nm to between 60 and 70nm and the $P(\theta)^{-1}$ curve becomes compatible with the toroidal model. The only change in sedimentation coefficient at this point is a small increase. As suggested above this insensitivity of the hydrodynamic technique is possibly explained by a change in the free-draining properties of the molecule and such a hypothesis would fit well with the observed transition to the compact toroid at $\sigma = -0.018$ (−9 superhelical turns) as this structure would intuitively be expected to be less free-draining and more flexible than the rigid Y-shaped molecule. Thus two opposing forces combine to make the alteration in sedimentation very small.

From $\sigma = -0.017$ the root-mean-square radius increased monotonically to a value of 120nm at $\sigma = 0$ at the open circular conformation; the increase in this value over the one of 109.4nm for RF II DNA without dye (Jolly & Campbell, 1972*c*) is presumably due to the extension of the molecule by dye intercalation. At these values of superhelix density no models were very good although the toroid error limits were always nearer the experimental values. It seems likely here

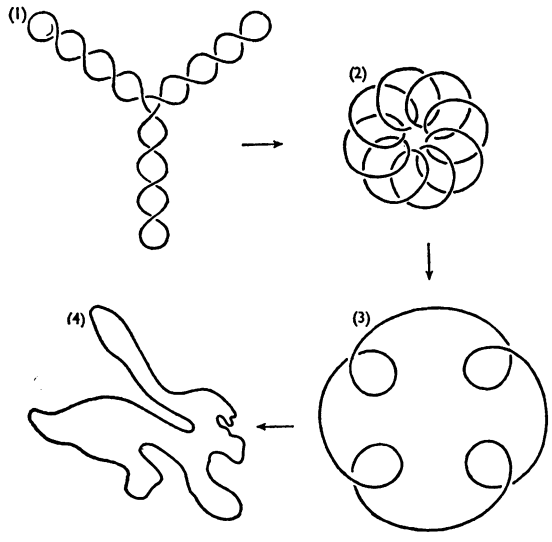

Fig. 14. *Projected structure transitions of $\phi X174$ RF I DNA as the number of supercoils (τ) decreases from 12 to zero*

(1) $\tau = -12$, $\sigma = -0.025$; rigid interwound extended Y shape. (2) $\tau = -8$, $\sigma = -0.017$; fairly rigid very compact toroid-like structure. (3) $\tau = -4$, $\sigma = -0.080$; flexible looped circle. (4) $\tau = 0$, $\sigma = 0$; open circular form.

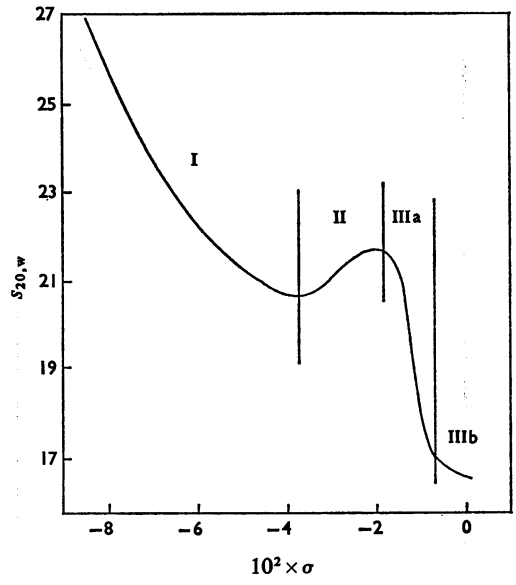

Fig. 15. *Scheme of the behaviour of the sedimentation coefficient of supercoiled DNA as a function of superhelix density*

This is based on the results of Upholt *et al.* (1971) for SV40 DNA (mol.wt. 3.1×10^6). Similar results were obtained for bacteriophage PM2 and bacteriophage λ b_2b_5c DNA. The curve is at least triphasic, possibly quadrophasic. These phases are delineated approximately as follows: I, below $\sigma = -0.035$; II, from $\sigma = -0.035$ to -0.017; IIIa, from $\sigma = -0.017$ to -0.005; IIIb, from $\sigma = -0.005$ to 0.

that the structure deviates from an exact toroid and flattens somewhat. It will also be becoming more flexible, making rigid models inapplicable. As σ decreases to zero the toroid turns can be expected to come out uniformly so that the molecule goes through a looped circle conformation to an open circle. There are no good models available for this state with which to construct $P(\theta)^{-1}$ curves for comparison with experimental values except at the open circular configuration.

Upholt *et al.* (1971) have obtained curves of the form of Fig. 15 for SV40, bacteriophage PM2 and bacteriophage λ b_2b_5c DNA. They concluded: (*a*) as supercoils were introduced in region IIIb to about $\sigma = -0.005$ there was little effect on the molecule and the hydrodynamic volume remained the same; (*b*) in region IIIa to the maximum at the boundary with region II the superhelical loops decreased the root-mean-square radius in a spherically coiled form thus increasing the sedimentation; (*c*) region II corresponded to a gradual change from a spherically coiled form to a tightly wound linear form; (*d*) the transition from region II to region I represented a transition to branched Y forms.

The results obtained here disagree slightly with (*a*) in that some contraction of the dimensions of the molecule has been observed in this region. Proposition (*b*) seems very reasonable and coincides with the conclusions reached here. However, proposition (*c*) is in conflict with the results here; our results suggest a rapid and direct transition from a spherically coiled toroidal form to a Y structure with further tightening of the Y structure in region II and a masking of this effect in the ultracentrifuge by alteration in the free-draining properties of the molecule. Thus the rigid straight interwound form never seems to exist in solution. Although there is no information here, it seems likely that the transition from regions II to I represents further branching to, say, H shapes. Branching has also been invoked to explain the sedimentation behaviour of normal supercoiled bacteriophage λ DNA (Hinton & Bode, 1971), which is presumably in region II as are all naturally occurring DNA molecules (Wang, 1969). Thus it seems that electron micrographs must be extrapolated with extreme caution to solution conditions. The use of included controls, such as normal bacteriophage

PM2 DNA by Upholt *et al.* (1971) can help monitor individual variations in electron micrographs but cannot help in the interpretation of results with respect to solution structure. The almost universally used protein monolayer method of Kleinschmidt & Zahn (1959) for preparing the electron micrographs subjects the molecules to strong spreading forces to ensure that the molecules are clearly visible by eliminating three-dimensional coiling due to thermal fluctuations. This process, however, obviously distorts molecules with respect to solution and could easily be imagined, for example, to pull out a Y structure into a linear form. These points are not new and have been discussed in some detail (Kleinschmidt *et al.*, 1965; Vinograd *et al.*, 1968). A particularly confusing situation has been found by Wang (1969) where the effect of ionic strength on the number of superturns in closed cyclic bacteriophage λ DNA as examined by electron microscopy (Bode & MacHattie, 1968) seemed different in magnitude and sign from that found by Wang (1969) from hydrodynamic experiments.

Forces affecting structural transitions

It is possible now to attempt some simple thermodynamic calculations on these structures and transformations outlined above. Bauer & Vinograd (1970) have given an equation for the free energy of supercoiling, G_{sc}, which is:

$$G_{sc}/RT = 0.88\tau^2 - 0.038\tau^3 \quad (1)$$

where R is the gas constant, T the absolute temperature and τ the number of superhelical turns. Davidson (1972) has generalized this, by using intensive quantities, to an equation that is generally applicable, which is:

$$g(\sigma)/RT = 422\sigma^2 - 880\sigma^3 \quad (2)$$

where $g(\sigma)$ is the free energy of supercoiling per ten base pairs; in addition he states that G_{sc} has, in general, three components: (*a*) the energy of bending for the double helix, G_b; (*b*) the torsional energy, G_t; (*c*) energy due to interactions between topologically distant segments in the contorted supercoiled conformation, G_i; this last is probably small.

Gray & Hearst (1968) have derived an expression linking the free energy of bending a DNA molecule with its curvature and persistence length by equating the continuous homogeneous thread model of Landau & Lifshitz (1958) with Kratky & Porod's (1949) worm-like coil model. This can be written:

$$G_b = RTlZp^2/2 \quad (3)$$

where l is the contour length, Z the persistence length, and p is the curvature; for a curve wound as a helix round a cylinder of values r at a pitch angle a, $p = \cos^2 a/r$ (Fuller, 1971).

Applying these equations at $\sigma = -0.025$ (−12 superhelical turns, Y-shaped molecule) $G_{sc} = 78$ kcal/mol of DNA. By using the dimensions of the various models dictated by the root-mean-square radius etc. (Jolly & Campbell, 1972*a*), G_b (Y shape) = 21 kcal/mol, G_b (toroid) = 73 kcal/mol and G_b (straight interwound) = 72 kcal/mol, if Z is taken as 41 nm (Jolly & Campbell, 1972*c*; Triebel *et al.*, 1971; Hearst *et al.*, 1968). Thus, even from these simple considerations the Y shape appears energetically more likely, although the calculations are approximate and assume constant curvature. At $\sigma = -0.018$ (−9 superhelical turns) the other point where a feasible model was found, $G_{sc} = 43$ kcal/mol (with $\tau = -9$) and $G_b = 20$ kcal/mol for the toroid and interwound models; thus the decisive factor in favour of the toroid is probably G_t. Fuller (1971), with an elastic rod as a model for the DNA duplex and, in effect, considering only G_b and G_t, has derived an energy expression for the rod twisted into a supercoil. It can be written:

$$G_{sc} = \tfrac{1}{2}A\,lp^2 + 2\pi^2 C(\beta)^2/l \quad (4)$$

where A is the coefficient of flexural rigidity, C is the coefficient of torsional rigidity, and β is the number of duplex turns. The first expression on the right-hand side is exactly equivalent to G_b, the second to G_t. Attempts to use eqn. (4), however, were hampered by the fact that the quantity β is not known, as $\tau+\beta$ has been previously assumed absolutely constant for the dye titration to evaluate (Wang, 1969). In addition C must alter with β, since when $\beta = 487$ (B structure of DNA) $G_t = 0$ and hence C must be zero.

One calculation was attempted; if $\beta = \beta_{12}$ at $|\tau| = 12$, $\beta = \beta_9$ at $|\tau| = 9$, G_i is assumed zero and C assumed constant over this range, then by using eqn. (4) at $|\tau| = 12$ and 9, $\beta_{12}/\beta_9 = 1.55$. As this implies massive changes in the duplex winding, this seems impossible. Thus either G_i is not negligible or C has changed. The latter seems very possible as in the toroidal model the right-hand duplex is curving in a left-handed superhelix whereas in the Y-shaped model it curves in a right-handed superhelix. Thus the torsional restraints probably alter in a complex manner as the DNA moves from the Y shape at −10 superhelical turns to the toroid at −9 superhelical turns. Crick (1971) has pointed out that the right-handed duplex will prefer to take up a left-handed superhelix, other forces being equal.

Effect of proflavine on persistence length

In considering the $P(\theta)^{-1}$ and persistence length of RF I DNA titrated with proflavine hemisulphate to an open circular form a number of additional factors must be taken into account. First, the titration may not be exact and some small torsion may remain

in the DNA duplex; there is no real way of checking this and it might be expected to decrease by a small amount the dimensions of the molecule, thus apparently decreasing the persistence length. Secondly, in calculating the $P(\theta)^{-1}$ function it was assumed that each dye molecule bound intercalated and lengthened the duplex by 0.335nm (Drummond *et al.*, 1966); however, it has been suggested that not all the bound proflavine intercalates (Ramstein *et al.*, 1972). This would mean an overestimation of the molecular contour length in the theoretical $P(\theta)^{-1}$, and again an underestimation of the persistence length. This effect seems likely to be very small, especially in view of the clear-cut spectrophotometric isosbestic points obtained. In Fig. 8, the points for the titrated RF I DNA are higher than those for RF II DNA, indicating a more-extended molecule, as do the relative root-mean-square radii. However, when the extension owing to intercalation is allowed for, the persistence length does seem to have fallen (from 41nm to 36 ± 3nm) on the binding of dye. Although this is the effect the above errors would have, their effects seem unlikely to be as large as this [e.g. in Fig. 11, curve 4 ($r=0.052$) is not far from curve 5 ($r=0.06$)], and the qualitative conclusion is made that dye intercalation makes DNA more flexible. Bauer & Vinograd (1970) have also suggested this on the basis of the asymmetry of the free energy of supercoiling with respect to the sign of τ calculated from ethidium bromide-binding experiments, and Lloyd *et al.* (1968) have found this also from direct hydrodynamic experiments. Mauss *et al.* (1967) found that at high values of bound dye (>0.13mol of dye/mol equiv. of nucleotide) the persistence length increased. However, their approach was not exact and there is some indication from their results, that at low amounts of bound dye the persistence length decreases.

Biological relevance of structural transitions

The main aim of this study has been to visualize the structural problems implicit in terms of replication and transcriptions of circular DNA molecules. The points at which large structural transitions occur could be topological triggers for specific biological processes. In general terms supercoiling clearly plays a role in the replication of closed circular DNA and has been suggested as a control mechanism in the replication of λ bacteriophage (Dove *et al.*, 1971). Supercoiled molecules are also known to have different transcriptional properties. Thus SV40 DNA form I is transcribed asymmetrically *in vitro* whereas form II is transcribed symmetrically (Westphal, 1970). *In vivo* the early RNA is transcribed asymmetrically but the total RNA symmetrically (Lindstrom & Dulbecco, 1972; Khoury *et al.*, 1972). Hence supercoiling in this case is an important control factor. There seems little doubt that during the transcription process the supercoil goes through the toroidal transformation as a sizeable fraction of the product RNA is hybridized into its supercoil template (Hayashi, 1965).

Individual proteins can also induce the toroidal transformation. Thus the ω protein of Wang (1971) is known to decrease but not to abolish superhelical turns and it is possible that proteins which induce the A structure of DNA, such as the arginine-rich histone of Shih & Fasman (1971), could cause this structural change. It is therefore relevant to examine these two forms of DNA, the Y shape and the toroid, to see if their tertiary structure could limit or alter functions such as replication and transcription. In the Y shape the DNA strands are much closer to each other and access for large proteins might be limited except at the three ends of the arms. In the toroid the DNA strands are not so close to each other at any point and access through its massive loops may be easier. In terms of secondary structure, although the differences detectable are slight (Campbell & Lochhead, 1971), there must be a considerable strain at the loops at the ends of the Y shape that could lead to small localized changes in secondary structure. The toroidal model has a more even distribution of torsional strain but the superhelical torque has changed to a left-handed one which may affect secondary structure in a different manner. Thus the structural changes described may play some small role in the biological properties of superhelical DNA.

We should like to acknowledge the help of Dr. K. Sargeant of the Microbiological Research Establishment at Porton, Wiltshire for the provision of bacteriophage-infected cells. We are also grateful to the late Professor J. N. Davidson, F.R.S. and Professor R. M. S. Smellie for their interest and for providing facilities with the aid of a grant from the Cancer Research Campaign. The Fica 50 scattering instrument was obtained with a grant from the Science Research Council. D. J. J. was in receipt of a Medical Research Council research studentship.

References

Bauer, W. & Vinograd, J. (1968) *J. Mol. Biol.* **33**, 141–171
Bauer, W. & Vinograd, J. (1970) *J. Mol. Biol.* **47**, 419–435
Berry, G. C. (1966) *J. Chem. Phys.* **44**, 4550–4564
Blake, A. & Peacocke, A. R. (1968) *Biopolymers* **6**, 1225–1253
Bloomfield, V. A. (1966) *Proc. Nat. Acad. Sci. U.S.* **55**, 717–720
Bode, V. C. & MacHattie, L. A. (1968) *J. Mol. Biol.* **32**, 673–679
Campbell, A. M. & Jolly, D. J. (1972) *Biochem. J.* **127**, 39P–40P
Campbell, A. M. & Lochhead, D. S. (1971) *Biochem. J.* **123**, 661–663
Cohen, G. & Eisenberg, H. (1969) *Biopolymers* **8**, 45–55

Crawford, L. V. & Waring, M. J. (1967) *J. Mol. Biol.* **25**, 23–30
Crick, F. H. C. (1971) *Nature (London)* **234**, 25–27
Davidson, N. (1972) *J. Mol. Biol.* **66**, 307–309
Dawson, J. R. & Harpst, J. A. (1971) *Biopolymers* **10**, 2499–2508
Dean, W. W. & Lebowitz, J. (1971) *Nature (London) New Biol.* **231**, 5–8
Dove, W. F., Inokucji, M. & Stevens, W. F. (1971) in *The Bacteriophage Lambda* (Hershey, A. D., ed.), pp. 747–771, Cold Spring Harbor Laboratory, New York
Drummond, D. S., Pritchard, N. J., Simpson-Gildermeister, V. F. W. & Peacocke, A. R. (1966) *Biopolymers* **4**, 971–987
Eisenberg, H. & Felsenfeld, G. (1967) *J. Mol. Biol.* **30**, 17–37
Flory, P. J. (1953) *Principles of Polymer Chemistry*, Cornell University Press, Ithaca
Flory, P. J. (1969) *Statistical Mechanics of Chain Molecules*, Interscience, New York
Follet, E. A. C. & Crawford, L. V. (1967) *J. Mol. Biol.* **28**, 455–459
Freifelder, D. (1970) *J. Mol. Biol.* **54**, 567–577
Fukatsu, M. & Kurata, M. (1966) *J. Chem. Phys.* **44**, 4539–4545
Fuller, F. B. (1971) *Proc. Nat. Acad. Sci. U.S.* **68**, 815–819
Geiduschek, E. P. & Holtzer, A. (1958) *Advan. Biol. Med. Phys.* **6**, 431–551
Gersch, N. F. & Jordan, D. O. (1965) *J. Mol. Biol.* **13**, 138–156
Glaubiger, D. & Hearst, J. E. (1967) *Biopolymers* **5**, 691–696
Gray, H. B. & Hearst, J. E. (1968) *J. Mol. Biol.* **35**, 111–129
Haugen, G. R. & Melhuish, W. H. (1964) *Trans. Faraday Soc.* **60**, 386–394
Hayashi, M. (1965) *Proc. Nat. Acad. Sci. U.S.* **54**, 1736–1743
Hearst, J. E., Schmid, C. W. & Rinehart, F. P. (1968) *Macromolecules* **1**, 491–494
Helinski, D. M. & Clewell, D. B. (1971) *Annu. Rev. Biochem.* **40**, 899–942
Hinton, D. M. & Bode, V. C. (1971) *Fed. Proc. Fed. Amer. Soc. Exp. Biol.* **30**, 1095
Hirschman, S. Z. & Felsenfeld, G. (1966) *J. Mol. Biol.* **16**, 347–358
Jolly, D. J. & Campbell, A. M. (1972*a*) *Biochem. J.* **128**, 569–578
Jolly, D. J. & Campbell, A. M. (1972*b*) *Biochem. J.* **129**, 42P
Jolly, D. J. & Campbell, A. M. (1972*c*) *Biochem. J.* **130**, 1019–1028
Khoury, G., Byrne, J. C. & Martin, M. A. (1972) *Proc. Nat. Acad. Sci. U.S.* **69**, 1925–1928
Kilkson, R. & Maestre, M. F. (1962) *Nature (London)* **195**, 494–495
Kleinschmidt, A. K. & Zahn, R. K. (1959) *Z. Naturforsch. B* **14**, 770–779
Kleinschmidt, A. K., Burton, A. & Sinsheimer, R. L. (1963) *Science* **142**, 961
Kleinschmidt, A. K., Kass, S. J., Williams, R. C. & Knight, C. A. (1965) *J. Mol. Biol.* **13**, 749–756
Krasna, A. I. (1970) *Biopolymers* **9**, 1029–1038
Kratky, O. & Porod, G. (1949) *Rec. Trav. Chim. Pays-Bas* **68**, 1106–1122
Landau, L. & Lifshitz, G. (1958) *Statistical Physics*, pp. 478–482, Pergamon Press, London
Lindstrom, D. M. & Dulbecco, R. (1972) *Proc. Nat. Acad. Sci. U.S.* **69**, 1517–1520
Lloyd, P. H., Prutton, R. N. & Peacocke, A. R. (1968) *Biochem. J.* **107**, 353–359
Luzzati, V. & Nicolaieff, A. (1963) *J. Mol. Biol.* **7**, 142–163
Mauss, Y., Chambron, J., Daune, M. & Benoit, H. (1967) *J. Mol. Biol.* **27**, 579–589
Pardon, J. F., Wilkins, M. F. H. & Richards, B. M. (1967) *Nature (London)* **215**, 508–509
Peacocke, A. R. & Skerret, J. N. H. (1956) *Trans. Faraday Soc.* **52**, 261–279
Ramstein, J., Dourlent, M. & Leng, M. (1972) *Biochem. Biophys. Res. Commun.* **47**, 874–882
Revet, B. M. J., Schmir, M. & Vinograd, J. (1971) *Nature (London) New Biol.* **229**, 10–13
Rhoades, M. & Thomas, C. A. (1968) *J. Mol. Biol.* **37**, 41–61
Saucier, J. M., Festy, B. & Le Pecq, J. B. (1971) *Biochimie* **53**, 973–980
Schmid, C. W. & Hearst, J. E. (1969) *J. Mol. Biol.* **44**, 143–160
Schmid, C. W., Reinhart, F. P. & Hearst, J. E. (1971) *Biopolymers* **10**, 883–893
Shih, T. Y. & Fasman, G. D. (1971) *Biochemistry* **10**, 1675–1683
Sinanoglu, O. & Abdulnur, S. (1964) *Photochem. Photobiol.* **3**, 333–342
Sinsheimer, R. L. (1959) *J. Mol. Biol.* **1**, 43–53
Studier, F. W. (1965) *J. Mol. Biol.* **11**, 373–390
Tanford, C. (1961) *Physical Chemistry of Macromolecules*, p. 151, Wiley, New York
Triebel, H., Reinert, K. E. & Strassburger, J. (1971) *Biopolymers* **12**, 2619–2621
Upholt, W. B., Gray, H. B. & Vinograd, J. (1971) *J. Mol. Biol.* **62**, 21–38
Utiyama, H. & Doty, P. (1971) *Biochemistry* **10**, 1254–1264
Vinograd, J. & Lebowitz, J. (1966) *J. Gen. Physiol.* **49**, 103–125
Vinograd, J., Lebowitz, J., Radloff, R., Watson, R. & Lapais, P. (1965) *Proc. Nat. Acad. Sci. U.S.* **53**, 1104–1111
Vinograd, J., Lebowitz, J. & Watson, R. (1968) *J. Mol. Biol.* **33**, 173–197
Wang, J. C. (1969) *J. Mol. Biol.* **43**, 263–272
Wang, J. C. (1971) *J. Mol. Biol.* **55**, 523–533
Waring, M. J. (1965) *J.Mol.Biol.* **13**, 269–282
Waring, M. J. (1970) *J. Mol. Biol.* **54**, 247–279
Westphal, H. (1970) *J. Mol. Biol.* **50**, 407–420
Zimm, B. H. (1948) *J. Chem. Phys.* **16**, 1093–1116

APPENDIX

Theoretical Models

Theoretical particle-scattering factors, $P(\theta)$, were calculated from the equation:

$$P(\theta) = \frac{1}{N^2}\sum_{n}^{N}\sum_{m}^{N}(\sin hr_{nm}/hr_{nm}) \qquad (1)$$

where N is the total number of scattering points in the molecule, h is $4\pi\sin(\theta/2)/\lambda'$ (θ being the angle at which the scattered intensity is observed), r_{nm} is the absolute value of the vector between scattering points n and m (Geiduschek & Holtzer, 1958) and λ' is the wavelength of light in solution. The summations were carried out by computer over all n and m for the defined geometric models dictated by the root-mean-square radius, molecular contour length and number of superhelical turns, assuming them to be rigid, which are shown in Figs. 5(*a*) and 5(*b*) of the main paper (Campbell & Jolly, 1973), i.e. the straight interwound with large radius and the compact toroid. The numbers of integral superhelical turns were taken as −9, −8 and −7, as obtained from the number of superhelical turns at 25°C of −11.8 from ethidium bromide titration (Jolly & Campbell, 1972), a linear mass density of 1950 daltons/nm was assumed i.e. the DNA was assumed to be in the B structure (Campbell & Lochhead, 1971), and the effect of errors assessed by calculating curves for the models by using maximum error data.

Straight interwound model

For this model (Fig. 5*a* of the main paper), the superhelix radius has become much too large to treat it as a simple rod and therefore the formulation of Gray (1967) was used to describe it.

The geometrical representation of the model is shown in Fig. 5 of the main paper. The molecule is considered, neglecting end effects, as two interwound helices each with one-half the contour length of the molecule with the z axis equivalent to the superhelix axis and the two helices beginning 180° apart in a plane parallel to the x–y plane. The parametric equations for a helix are then:

$$\begin{aligned} x &= (\cos t)\,d/2 \\ y &= (\sin t)\,d/2 \\ z &= pt/2 \end{aligned} \qquad (2)$$

where d is the superhelix diameter, t is the polar angle in the x–y plane and p is the superhelix pitch.

The intersegment distances, r_{nm}, fall into two categories: interhelix distances when n and m are on different helices and intrahelix distances when they are on the same helix. Then, for interhelix distances:

$$r_{nm}^2 = 2r^2\{1-\cos[(n-m)\,t_b-\pi]\} + (p^2/4\pi^2)\,[(n-m)\,t_b]^2 \qquad (3a)$$

and for intrahelix distances:

$$r_{nm}^2 = 2r^2\{1-\cos[(n-m)\,t_b]\} + (p^2/4\pi^2)\,[(n-m)\,t_b]^2 \qquad (3b)$$

where t_b is the projection in the x–y plane of the angle between adjacent segments and is $2\arcsin(\pi K/N)$ and τ is the number of superhelical turns. Therefore:

$$P(\theta)^{-1} = 2/N^2\left[\sum_{n}^{N/2}\sum_{m}^{N/2}\frac{\sin hr_{nm}}{hr_{nm}}\right](\text{interhelix}) + \sum_{n}^{N/2}\sum_{m}^{N/2}\frac{\sin hr_{nm}}{hr_{nm}}(\text{intrahelix}) \qquad (4)$$

where h, r_{nm} and N are as in eqn. (1). The equation:

$$p^2 = (P/\tau)^2 - (\pi d)^2 \qquad (5)$$

where P is the contour length, relates these quantities. The procedure was to use the eqn.:

$$Rg^2 = \frac{1}{2N^2}\sum_{n=1}^{N}\sum_{m=1}^{N} r_{nm}^2$$

(Tanford, 1961) to calculate the root-mean-square radius, Rg, from a specified superhelix diameter and vary this by trial and error until the calculated Rg matched the experimental. The dimensions thus specified were used to calculate $P(\theta)$ values from eqn. (4) by computer summation.

Toroid model

The $P(\theta)^{-1}$ curve for this model (Fig. 5*b* in the main paper) was calculated for the dimensions dictated by Rg, exactly as described previously (Jolly & Campbell, 1972).

References

Campbell, A. M. & Jolly, D. J. (1973) *Biochem. J.* **133**, 209–225

Campbell, A. M. & Lochhead, D. S. (1971) *Biochem. J.* **123**, 661–663

Geiduschek, E. P. & Holtzer, A. (1958) *Advan. Biol. Med. Phys.* **6**, 431–551

Gray, H. B. (1967) *Biopolymers* **5**, 1009–1019

Jolly, D. J. & Campbell, A. M. (1972) *Biochem. J.* **128**, 569–578

Tanford, C. (1961) *Physical Chemistry of Macromolecules*, p. 151, Wiley, New York